10th INTERNATIONAL SCIENTIFIC CONFERENCE
ON DEFENSIVE TECHNOLOGIES
OTEH 2022
Belgrade, Serbia, 13 – 14 October 2022

MEASUREMENT OF HOVER PERFORMANCES FOR MINI UNMANNED AIRCRAFT VEHICLE

MARIJA SAMARDŽIĆ
Military Technical Institute, Belgrade, marija.samardzic.vti@gmail.com

LAZAR PETROVIĆ
Military Technical Institute, Belgrade, lazar.petrovic.node@gmail.com

UROŠ IVKOVIĆ
Military Technical Institute, Belgrade, uske80@gmail.com

SNEŽANA ZUROVAC
Military Technical Institute, Belgrade, zurovac@medianis.net

Abstract: *This paper presents measurement of hover performances for quadcopter unmanned aircraft vehicle (UAV). The tests took place in the Experimental Aerodynamic Laboratory at Military Technical Institute, Belgrade. Mini unmanned aircraft vehicle DJI Phantom was chosen as a UAV test model. The main objective of the presented test was to measure forces and moments generated on the UAV model as a function of the rotors RPM. The UAV model was run through a range of defined rotors RPM numbers in hover mode. The rotors speed control were conducted to match the target RPM. The forces and moments were measured using internal six-component wind tunnel balance. To match expected values of the forces and moments, calibration of the six-component balance was done for two load ranges. The UAV model was modified from its typical consumer configuration to facilitate connection to the internal balance. Measurement of hover performances was performed on the calibration rig in the T-38 wind tunnel calibration laboratory.*

Keywords: *unmanned aircraft vehicle, hover performances, aerodynamic load, wind tunnel balance.*

1. INTRODUCTION

Mini unmanned aircraft vehicles are being used more and more every day. The areas of application can be various: from the use of recreational aviation enthusiasts to professional field recording for various purposes. The UAV of certain configurations, with the most advanced construction and performance, are also used for military purposes. One of the first indicators of the potential capabilities of an UAV is its payload. In addition to the appropriate flight characteristics, one of the most important parameters for evaluating the capability of an UAV is the weight of additional payload that the aircraft can carry. In the process of designing new or testing already existing UAV, the possibility of experimental determination of aerodynamic forces and moments as a function of the air speed, vehicle attitude and rotor speed is of great importance [1-4]. The most often, the first stage of such experiments is determination of the forces and moments on the UAV in the hover mode. This paper presents the measurements of the hover performance of a mini UAV in the calibration laboratory of the T-38 wind tunnel. The presented results are the first part of extensive testing, the continuation of which is planned in the small subsonic wind tunnel T-32. The main goal of the presented tests is to measure the normal force (thrust), in the hovering mode and verify the selection of the internal wind tunnel balance. This balance should enable the measurement of all six aerodynamic force components in the UAV model wind tunnel testing.

2. MINI UNMANNED AIRCRFAT VEHICLE MODEL

DJI Phantom aircraft is chosen for hover and wind tunnel testing, Figure 1. This is commercially available multicopter whose primary mission is photographic surveillance. The unmanned aircraft vehicle was modified from their original configuration to facilitate testing on the calibration rig and in theT-32 wind tunnel. The most significant changes were made in the internal electronics.

Figure 1. DJI Phantom aircraft

The basic quadcopter UAV physical characteristics are shown in Table 1 [5].

Table 1. The DJI Phantom physical characteristics

Parameters	Range
Operating temperature	from -10° to 50°C
Power consumption	3.12 W
Take-off weight	< 1200 g
Max ascent/descent speed	6 m/s
Max flight velocity	10 m/s
Diagonal distance (motor center to motor center)	350mm
Weight	670 g
Weight (with battery)	800 g

3. INTERNAL WIND TUNNEL BALANCE FOR THE MESUREMENTS OF THE AERODYNAMIC LOAD

In the Experimental Aerodynamic Laboratory at the Military Technical Institute, measurements of the aerodynamic load on the mini UAV models have not been performed so far. Selection of the suitable internal wind tunnel balance for measurements of the aerodynamic load is a very important step in conducting the experiment preparation. The dimensions and geometry of the wind tunnel balance should be such that it can be placed in a rather narrow space inside the model. The wind tunnel balance should also enable the measurement of the aerodynamic components with the required accuracy, taking into account that some components will have very small values.

The expected values of the aerodynamic load on the DJI Phantom model are determined based on the available published experimental results. The results of the tests on the six different UAV models are presented in the reference [6]. Table 2 shows the nominal flight weight for the tested six models.

Table 2. Model nominal flight weight [6]

Model	Nominal Flight Weight (including cameral payload) [N]
3DR SOLO	14.678
DJI Phantom 3	12.453
3DR Iris+	12.453
Drone America x8	56.923
Straight Up Imaging Endurance	26.682

One and the same six-axis load cell was used for all five aircraft shown in Table 2. Measuring range of the six-axis load cell is: 222 N in x- and y- direction (axial and side force), 444 N in z-direction (normal force) and maximum moments of 17 Nm (rolling moment, yawing moment and pitching moment). A load cell with a smaller measuring range was originally planned for testing lighter aircrafts. Due to appearance of large vibrations during the first wind tunnel tests on lighter model, the same six-axis load cell was used in the tests of all models [6].

Take-off weight for the model DJI Phantom is less than 11.8 N [5]. Based on this data, as well as on the measured data for models shown in Table 2, for testing of the DJI Phantom model 0.75 inch ABLE internal balance was selected. The six basic components of the balance consist of two normal force elements (*FN1* and *FN2*) for determination of normal force (*Z*) and pitching moment (*M*), two side force (*FS1* and *FS2*) for determination of side force (*Y*) and yawing moment (*N*), dual force element (FRX) for determination of axial force (X) and dual moment element (*FRL*) for determination of rolling moment (*L*), Figure 2.

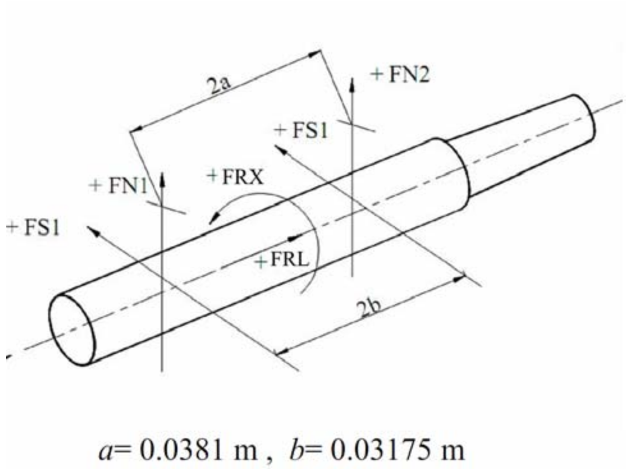

Figure 2. Basic component of the 0.75 inch ABLE internal balance

The calibration of the six-component balance was performed for two load ranges: nominal operating load range and reduced load range, Table 3. The calibration was performed on the calibration rig in the T-38 wind tunnel calibration laboratory, Figure 3. The balance calibration was consisted of the manual application of dead weights. This process was used for both positive and negative loadings at various stations along the calibration body. Summary of achieved accuracy of the calibration, as obtained in a checkout after the calculation of the calibration matrix, for both load ranges, is given in Table 4.

Table 3. The six-component balance load range

Nominal operating load range					
X [N]	*Y* [N]	*Z* [N]	*L* [Nm]	*M* [Nm]	*N* [Nm]
111	356	668	6.8	25	11
Reduced load range					
X [N]	*Y* [N]	*Z* [N]	*L* [Nm]	*M* [Nm]	*N* [Nm]
34	84	170	2.1	6.5	2.7

Figure 3. The six-component balance on the T-38 calibration rig

Table 4. Summary of achieved accuracy of the balance calibration

Nominal operating load range						
Component	*X*	*Y*	*Z*	*L*	*M*	*N*
Err. [N, Nm]	0.312	1.033	-0.527	0.028	0.037	0.039
P. Err. [%]	0.281	0.290	-0.079	0.411	0.146	00.352
Std.d. [%]	0.083	0.057	0.020	0.081	0.030	0.068
Reduced load range						
Component	*X*	*Y*	*Z*	*L*	*M*	*N*
Err. [N, Nm]	-0.116	-0.161	0.144	-0.017	0.026	0.014
P. Err. [%]	-0.341	-0.192	0.084	-0.798	0.398	0.518
Std.d. [%]	0.117	0.045	0.023	0.153	0.068	0.112

In Table 4 are:
Err. – maximum difference between applied and measured load,
P.Err. – maximum difference between applied and measured load calculated in relation to the component full scale,
Std.d – standard deviation of the errors calculated in relation to the component full scale.

In the measurements of hover performances of the DJI Phantom calibration matrix for the balance reduced load ranges was used.

4. MODEL MOUNTING ON THE CALIBRATION RIG

Measurements of the UAV test model aerodynamic characteristics were conducted with the model mounted on the calibration rig in the T-38 wind tunnel calibration laboratory, Figure 4. The camera gimbal mounting hole was used to support the model and serve as attachment points to the internal six-component balance.

Figure 4. DJI Phantom model in the T-38 wind tunnel calibration laboratory

The model is mounted on the internal six-component balance via suitable adapter. The six-component balance is connected via a cone to the sting, which is placed on the calibration rig, Figure 5. The same six-component balance and sting will be used for the testing of the DJI Phantom in the small subsonic wind tunnel T-32.

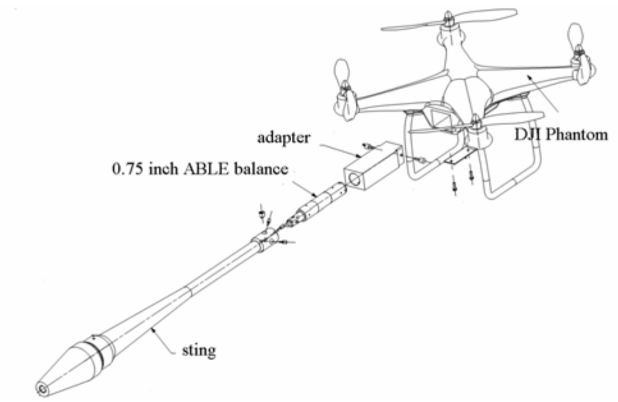

Figure 5. DJI Phantom model mounting

The DJI Phantom model mounted on the calibration rig is shown in Figure 6.

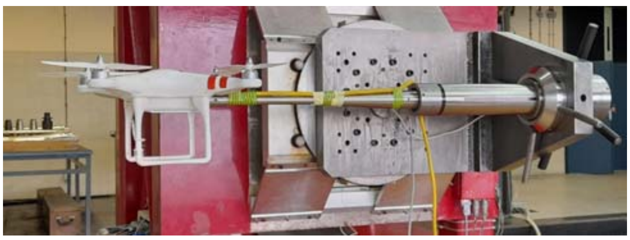

Figure 6. DJI Phantom model on the calibration rig

5. UAV SPEED CONTROL

The control of the number of revolutions of each drone engine is controlled by a central controller that receives data from sensors (GPS, electronic compass, altimeter, camera...), remote control and the current state of the engine and battery, and on the basis of that data determines whether the number of engine revolutions should be increased or decreased.

Testing the characteristics of the drone implies a constant number of revolutions of the engine during the measurement. The number of revolutions of the engine is the result of the state of all sensors, so it is not possible to achieve a constant number of revolutions of the engine using the remote control. Simulating the data of all the sensors that affect the engine's behavior would be a more demanding task than creating a computer-controlled controller individually for each engine.

In presented hover tests the required engine speeds as well as its characteristics are set using a computer. Speed measurement is performed optically or by sampling the voltage on one phase of the motor. The ESC management protocol used is the 50 Hz PWM Standard. The communication protocol between the PC and the interface is RS485. The microcontroller used was PIC12F1572. The control program was written in the C programming language and a compiler from the microcontroller manufacturer was used.

6. EXPERIMENTAL RESULTS

In hover test rotor RPM were varied in two ways. In the first part of the hover tests, the rotor speed was changed uniformly for all of the rotors on the model in order to quantify the effects of RPM on the model forces and moments, especially on the normal and axial forces. In the second part of the hover tests differential rotor speed was tested to measure moments on the vehicle. The moment centre is in the rotor plane at the point equidistant from all four rotors, Figure 7. The numbering of the rotors is shown in Figure 8.

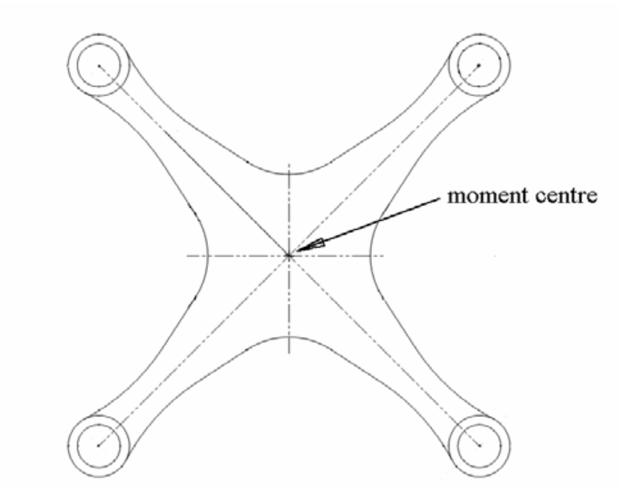

Figure 7. Moment centre

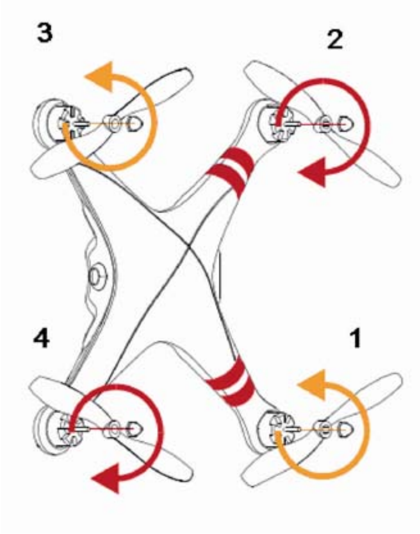

Figure 8. Rotor numbering [5]

The test matrix is presented in Table 5 and Table 6.

Table 5. Test matrix - uniform RPM

Uniform RPM				
Run number	RPM1	RPM2	RPM3	RPM4
1	4200	4200	4200	4200
2	4500	4500	4500	4500
3	4800	4800	4800	4800
4	5000	5000	5000	5000
5	5300	5300	5300	5300
6	5500	5500	5500	5500
7	6000	6000	6000	6000
8	6500	6500	6500	6500

Table 6. Test matrix - differential RPM

Differential RPM				
Run number	RPM1	RPM2	RPM3	RPM4
9	5300	0	0	0
10	0	5300	0	0
11	0	0	5300	0
12	0	0	0	5300
13	4200	4200	6400	6400
14	6400	6400	4200	4200
15	4200	6400	6400	4200
16	6400	4200	4200	6400

Measured forces and moments are reported in the axis system shown in Figure 9. The positive direction of the x-axis is from the moment centre toward the sting.

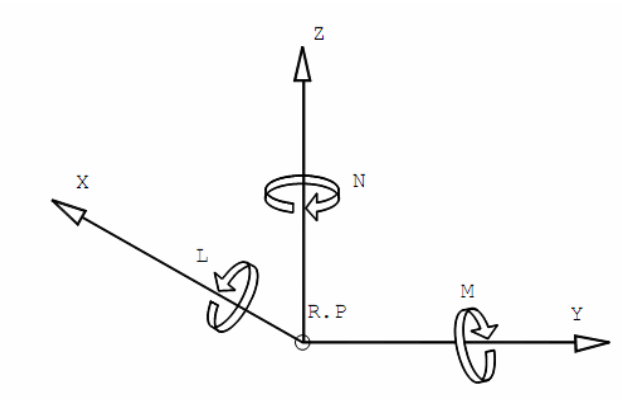

Figure 9. Directions of the forces and moments

Measured values of the normal force for the uniform rotor RPM is given in Table 7.

Table 7. Aerodynamic forces – uniform RPM

Uniform RPM	
Run number	Normal forces elements Normal force
1	RPM1=RPM2=RPM3=RPM4=4200
	FN1=4.4037N *FN2*=1.0777N *Z*=5.4814N
2	RPM1=RPM2=RPM3=RPM4=4500
	FN1=5.1341N *FN2*=1.3115N *Z*= 6.4456N
3	RPM1=RPM2=RPM3=RPM4=4800
	FN1=5.8540N *FN2*=1.4252N *Z*=7.2792N
4	RPM1=RPM2=RPM3=RPM4=5000
	FN1=6.3746N *FN2*=1.6476N *Z*=8.0222N
5	RPM1=RPM2=RPM3=RPM4=5300
	FN1=7.3449N *FN2*=1.3314N *Z*=8.6763N
6	RPM1=RPM2=RPM3=RPM4=5500
	FN1=8.0358N *FN2*=1.7496N *Z*= 9.7854N
7	RPM1=RPM2=RPM3=RPM4=6000
	FN1= 9.6877N *FN2*=2.1670N *Z*=11.8547N
8	RPM1=RPM2=RPM3=RPM4=6500
	FN1=11.5832N *FN2*=2.5297N *Z*= 14.1129N

Figure 10. shows the measured values of the normal force as a function of the rotors speed (rotor speed was changed uniformly for all of the rotors).

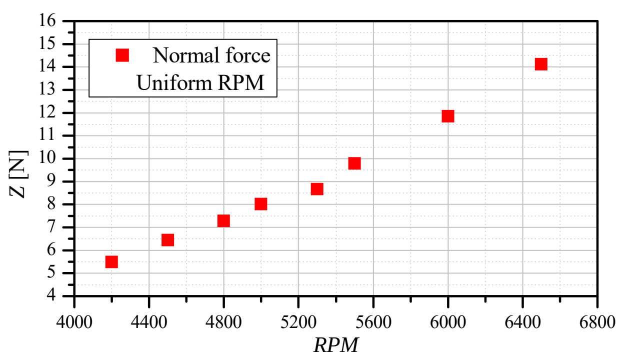

Figure 10. Normal force as a function of the RPM

Components of the aerodynamic load measured in the tests with differential rotors speed is shown in Table 8.

Table 8. Aerodynamic forces – differential RPM

Differential RPM						
Run number	*X* [N]	*Y* [N]	*Z* [N]	*L* [Nm]	*M* [Nm]	*N* [Nm]
9	RPM1=5300 RPM2=RPM3=RPM4=0					
	-0.09665	0.10291	2.34133	0.28509	-0.2994	0..06101
10	RPM2=5300 RPM1=RPM3=RPM4=0					
	-0.09023	-0.1867	2.4092	-0.2997	-0.3059	-0.06715
11	RPM3=5300 RPM1=RPM2=RPM4=0					
	0.02020	-0.1456	2.3722	-0.2994	0.2976	0.05209
12	RPM4=5300 RPM1=RPM2=RPM3=0					
	0.0053	0.1279	2.3535	0.2928	0.3063	-0.05255
13	RPM1=RPM2=4200 RPM3=RPM4=6400					
	-0.12564	-0.0004	9.48768	0.00349	0.44021	0.00734
14	RPM1=RPM2=6400 RPM3=RPM4=4200					
	-0.25343	-0.1156	9.79388	0.02840	-0.5469	-0.00777
15	RPM1=RPM4=4200 RPM2=RPM3=6400					
	-0.28165	-0.2162	9.66346	-0.4791	-0.0412	-0.01285
16	RPM1=RPM4=6400 RPM2=RPM3=4200					
	-0.12025	0.00155	9.80596	0.54010	-0.0292	0.00586

7. CONCLUSIONS

The main goal of the presented tests was to examine the possibility testing of mini unmanned aircraft vehicle in the Experimental Aerodynamic Laboratory at Military Technical Institute. This paper described the test setup of the mini UAV model in hover mode. The test generated data show that the defined test setup enables quality measurements of hover performance for mini UAV. The same test setup will be used to continue testing the mini UAV, which is planned in a small subsonic wind tunnel T-32.

ACKNOWLEDGEMENTS

This work was supported by the Ministry of Education, Science and Technological Development of the Republic of Serbia (Contract No. 451-03-68/2022-14/200325).

References

[1] THEYS,B., DIMITRADIS,G., ANDRIANNE,T., HENDRICK,P., De SCHUTTER,J.: *Wind Tunnel Testing of a VTOL MAV Propeller in Titled Operating Mode,* 2014 International Conference on Unmanned Aircraft Systems (ICAUS), 2014, pp.1064-1072.

[2] BARIS,E., BRITCHER,C.P., ALTAMIRANO,G.: *WIND Tunnel Testing of Static and Dynamic Aerodynamic Characteristics of a Quadricopter*, AIAA AVIATION 2019 Forum, June 17-21, 2019, Dallas, Texas, pp.1-12, AIAA 2019-2973

[3] SIMMA,M., MJOEN,H., BOSTROM,T.: *Measuring Wind Speed Using the Internal Stabilization System of Quadrotor Drone,* Drones, 23 (4), (2020), pp.1-10.

[4] BAZIN,J.M., FIELDS,T.D., SMITH,A.J.: *Feasibility of In-Flight Quadrotor Individual Motor Thrust Measurements,* AIAA Atmospheric Flight Mechanics Conference, January 4-8, 2016, San Diego, California, USA, pp. 1-12, AIAA 2016-1760

[5] PHANTOM Advance Manual, V1.4, DJI Innovations, 2013.03.22 Revision

[6] RUSSELL,C., WILLINK,G., THEODORE,C., JUNG,J., GLASNER,B.: *Wind Tunnel and Hover Performance Tests Results for Multicopter UAS Vehicle,* NASA/TM-2018-219758, Ames Research Center, 2018.